Journal Pre-proof

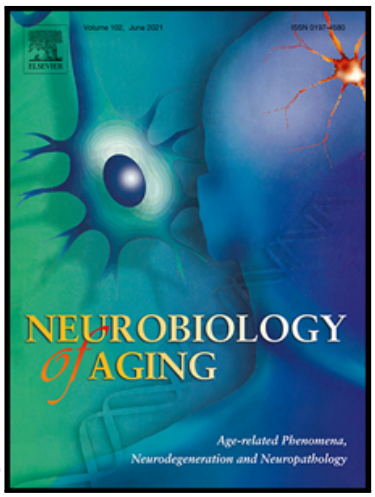

The canonical pattern of Alzheimer's disease atrophy is linked to white matter hyperintensities in normal controls, differently in normal controls compared to in AD

Joost M. Riphagen , Mahanand Belathur Suresh , David H. Salat , and the Alzheimer's Disease Neuroimaging Initiative (ADNI)

PII: S0197-4580(22)00029-X
DOI: https://doi.org/10.1016/j.neurobiolaging.2022.02.008
Reference: NBA 11321

To appear in: *Neurobiology of Aging*

Received date: 3 September 2021
Revised date: 16 February 2022
Accepted date: 19 February 2022

Please cite this article as: Joost M. Riphagen , Mahanand Belathur Suresh , David H. Salat , and the Alzheimer's Disease Neuroimaging Initiative (ADNI), The canonical pattern of Alzheimer's disease atrophy is linked to white matter hyperintensities in normal controls, differently in normal controls compared to in AD, *Neurobiology of Aging* (2022), doi: https://doi.org/10.1016/j.neurobiolaging.2022.02.008

This is a PDF file of an article that has undergone enhancements after acceptance, such as the addition of a cover page and metadata, and formatting for readability, but it is not yet the definitive version of record. This version will undergo additional copyediting, typesetting and review before it is published in its final form, but we are providing this version to give early visibility of the article. Please note that, during the production process, errors may be discovered which could affect the content, and all legal disclaimers that apply to the journal pertain.

© 2022 Published by Elsevier Inc.

Journal Pre-proof

- Vascular disease is strongly linked to the canonical pattern AD of atrophy
- WMH is correlated with lower cortical thickness in normal controls, less in AD
- Cortical loss in CN is co-localized with the canonical pattern of AD atrophy

Journal Pre-proof

Journal Pre-proof

The canonical pattern of Alzheimer's disease atrophy is linked to white matter hyperintensities in normal controls, differently in normal controls compared to in AD

Joost M. Riphagen, MD, PhD[a,b,d,*] jriphagen@mgh.harvard.edu, Mahanand Belathur Suresh, PhD[a,b,c], David H. Salat, PhD[a,b,e] and the Alzheimer's Disease Neuroimaging Initiative (ADNI)[#]

[a]Athinoula A. Martinos Center for Biomedical Imaging, Massachusetts General Hospital, Harvard Medical, School, Charlestown, MA, USA

[b]Department of Radiology, Massachusetts General Hospital, Harvard Medical School, Boston, MA, USA

[c]Department of Information Science and Engineering, Sri Jayachamarajendra College of Engineering, Mysuru, India

[d]Department of Psychiatry & Neuropsychology, Maastricht University, School for Mental Health & Neuroscience, Alzheimer Center Limburg, Maastricht, the Netherlands

[e]Neuroimaging Research for Veterans Center, VA Boston Healthcare System, Boston, MA, USA

[*]Corresponding author.

The authors declare no conflicts of interest.

[#]Data used in preparation of this article were obtained from the Alzheimer's disease Neuroimaging Initiative (ADNI) database (adni.loni.usc.edu). As such, the investigators within the ADNI contributed to the design and implementation of ADNI and/or provided data but did not participate in analysis or writing of this report. A complete listing of ADNI investigators can be found at: http://adni.loni.usc.edu

Abstract

White matter signal abnormalities (WMSA), either hypo- or hyperintensities in MRI imaging, are considered a proxy of cerebrovascular pathology and contribute to, and modulate, the clinical presentation of Alzheimer's disease (AD), with cognitive dysfunction being apparent at lower levels of amyloid and/or tau pathology when lesions are present. To what extent the topography of cortical thinning associated with AD may be explained by WMSA remains unclear. Cortical thickness group difference maps and subgroup analyses show that the effect of WMSA on cortical thickness in cognitively normal participants has a higher overlap with the canonical pattern of AD, compared to AD participants. (Age and sex matched group of 119 NC (AV45 PET negative, CDR=0) vs 119 participants with AD (AV45 PET positive, CDR >0.5). The canonical patterns of cortical atrophy thought to be specific to Alzheimer's disease are strongly linked to cerebrovascular pathology supporting a reinterpretation of the classical models of AD suggesting that a part of the typical AD pattern is due to co-localized cortical loss before onset of AD.

Keywords: Alzheimer's disease, vascular risk, white matter hyperintensities, cortical thickness, aging

Journal Pre-proof

White matter lesions can be detected using MRI using T1 (hypointense) and T2/FLAIR (hyperintense) weighted imaging or a combination of multiple sequences. These white matter signal abnormalities (WMSA) increase in prevalence as individuals age (de Leeuw et al., 2001) and more so in Alzheimer's disease (Lindemer et al., 2017a; Lindemer et al., 2015) are associated with cognitive dysfunction (Debette et al., 2007) and an increased risk of Alzheimer's disease (AD)(Birdsill et al., 2014; Mortamais et al., 2013). Prior work has shown that the presence of WMSA contribute to and modulate the clinical presentation of AD, with cognitive dysfunction being apparent at lower levels of amyloid and/or tau pathology when lesions are present suggesting that their presence may accelerate disease progression.(Birdsill et al., 2014 ; Debette et al., 2010; Lindemer et al., 2017b; Prins and Scheltens, 2015). While the underlying pathology of WMSA are still not fully understood, they are considered to be a proxy for vascular associated brain tissue damage (Brickman et al., 2015; Erten-Lyons et al., 2013; Gattringer et al., 2017; Kandel et al., 2016; Provenzano et al., 2013; Zhao and Gong, 2015). Imaging and post-mortem studies suggest that the link between WMSA, AD pathology and other dementias is different between brain areas (Desmarais et al., 2021; Garnier-Crussard et al., 2021; McAleese et al., 2021; McAleese et al., 2017; Rizvi et al., 2021; Van Etten et al., 2021). Prior studies have demonstrated that white matter lesions are associated with white matter alterations as measured with diffusion tensor imaging, an index of vascular health, in aging and AD (O'Sullivan et al., 2004) (Jacobs et al., 2013; Leritz et al., 2014; O'Sullivan et al., 2001; Riphagen et al., 2018; Vernooij et al., 2009). In addition, several studies reported a negative association between cortical grey matter volume and the burden of WMSA (Appelman et al., 2009; Capizzano, 2004; Godin et al., 2009; Knopman et al., 2015). Likewise, WMSA load has been linked to alterations in cortical thickness (Rizvi et al., 2018; Tuladhar et al., 2015; Wen et al., 2006). WMSA have been shown to be particularly associated with typical-AD and Limbic predominant AD-subtypes (Cedres et al., 2020; Ferreira et al., 2018). However, to what extent the topography of cortical thinning associated with AD may be explained by WMSA remains unclear.

showing associations with WMSA and spatial patterns of thinning due to AD (Belathur Suresh et al., 2018; Dickerson et al., 2009). To do so, we examined associations between WMSA and thickness in cognitively unimpaired amyloid negative older adults and compared spatial patterns to the canonical spatial patterns of AD cortical thinning derived from group comparisons of amyloid positive AD to amyloid negative cognitively unimpaired individuals from the neuroimaging initiative (ADNI) in age and sex matched groups.

2. Materials and Methods

2.1 Dataset

Data used in this article were obtained from the Alzheimer's disease neuroimaging initiative (ADNI) database (adni.loni.usc.edu). The ADNI was launched in 2003, led
by Principal Investigator Michael W. Weiner, MD. The main goal of the ADNI is to test whether magnetic resonance imaging, positron emission tomography, other biological markers, and clinical and neuropsychological assessment can be combined to measure the progression of MCI and AD. For up-to-date information, see www.adni-info.org.

We used the structural brain MRI scans from the Alzheimer's disease Neuroimaging Initiative (ADNI-2) dataset (adni.loni.usc.edu). Informed consent was obtained from all participants in this study.

2.2 Participants

A total of 403 participants (267 controls (CN) and 136 participants with an Alzheimer's disease diagnosis (AD) according to the ADNI criteria (subjective memory concern, abnormal memory function on education adjusted Logical memory II subscale of the Wechsler memory scale, MMSE between 20-26, CDR 0.5 or 1 and the NINCDS/ADRDA criteria for probable AD (McKhann et al., 2011)) were considered for this study. In addition to these criteria, we used biomarker information to exclude individuals with atypical patterns of AD pathology that might complicate the interpretation of results. Specifically, we chose participants with an AD diagnosis that where amyloid positive based on a Florbetapir (AV45) cutoff of 1.11 SUVR using the whole cerebellum as reference region and had a CDR

Journal Pre-proof

Florbetapir (AV45) levels below cutoff to minimize any AD pathology contributions of WMSA associations with cortical thickness. To ensure that co-variates that are related to age are balanced between groups, and the age difference between CN and AD groups did not drive effects, Optimal full matching was performed using the MatchIt package (Ho et al., 2011) in R, which calls functions from the Optmatch package (Hansen and Klopfer, 2006). Full matching is optimal with regards to minimizing a weighted average of the estimated distance measure between each treated subject and each control subject within each subclass.

2.3. Biomarker assessment

^{18}F-AV-45 Florbetapir positron emission tomography measures were used to quantify levels of neocortical Aβ. The duration of positron emission tomography imaging was 20 minutes and started 50 minutes after injection of tracer fluid. The neocortical standardized uptake value ratio is the mean uptake in an aggregate of the frontal lobe, cingulate cortex, lateral parietal, and lateral temporal regions relative to mean uptake in the whole cerebellum, including white and gray matter. Further processing of positron emission tomography images occurred as is described in a previous report (Landau et al., 2012). Participants were characterized as Aβ-positive if they exceeded the cutoff value of 1.11 standardized uptake value ratio, as previously determined in ADNI cohorts (Landau et al., 2012). For all the analyses mapped to the cortical surface all variables were used as a continuous rather than a dichotomized measure.

Journal Pre-proof

2.4. MRI acquisition.

Standard 3T baseline T1-weighted images were included from the ADNI data set. More detailed descriptions of the acquisition parameters are described elsewhere (Jack Jr. et al., 2008). Structural T1-weighted gradient echo pulse sequence data with dimensions of 170*256*256 mm with a voxel resolution of 1.2*1*1 mm were acquired in sagittal orientation with a repetition time of 2300 ms, echo time of 2.95 ms, flip angle of 9° and slice thickness

9000 ms, echo time of 90 ms, flip angle 150° and 5mm slice thickness.

2.5 Surface based cortical thickness analysis

The FreeSurfer image analysis suite version 5.3.0 (http://surfer.nmr.mgh.harvard.edu) was employed to process the MRI data and compute cortical thickness measurements. The technical details of cortical reconstruction and volumetric segmentation performed with the Freesurfer are described in prior publications (Fischl et al., 2004a; Fischl et al., 2004b). All images were visually checked after processing and if necessary, edited for errors in automatic skull stripping or estimation of the gray/white matter boundaries before reprocessing.

Cortical thickness measures were mapped on both the white matter border for easier orientation or on the inflated surface of each participant's reconstructed brain to allow visualization across the surface without interference from cortical folding. Maps were smoothed using a circularly symmetric Gaussian kernel with a full width half maximum (FWHM) of 20mm or 10mm and averaged across participants using a non-rigid high-dimensional spherical averaging method to align cortical folding patterns. This procedure provided accurate matching of morphologically homologous cortical locations among participants based on each individual's anatomy while minimizing metric distortion. This results in a mean measure of cortical thickness at each point on the reconstructed surface.

2.4 WMSA methods

This study uses the white matter hyperintensity volumes available through the ADNI database, calculated from fluid attenuated inversion recovery (FLAIR) and combining this with T1-weighted images using a Bayesian segmentation method described elsewhere (Fletcher et al., 2012), we will refer to these values as white matter signal abnormalities (WMSA) as it uses both T1 (hypo-intensities) and Flair (hyperintensity) data. This WSMA measurement approach is based on a Bayesian approach to segmentation of high-resolution 3D T1 and FLAIR sequences. In brief, non-brain structures are excluded from the 3D T1 images using an automated atlas-based method. The FLAIR image is transformed to the 3D

performed using a modified Bayesian probability structure based WMSA map created from approximately 700 individuals with semi-automatic detection of WMSA followed by manual editing. Likelihood estimates of the native image are calculated through histogram.

segmentation and thresholding. Further description can be found in the ADNI reference documentation "Four Tissue Segmentation in ADNI II" (DeCarli. et al., 2013).

The WMSA volume was expressed as a proportion of intracranial volume relative to the average sample IVC ((WMSA/ICV) * 1346

mean IVC of total sample), with 1 unit added before log-transformation to create an approximately normal distribution for the analyses.

2.5 Statistical analyses

All further analyses were done in R version 3.5.1 (http://www.R-project.org.). Demographics are reported in means and standard deviations and groups were compared using Welch two-sample t-test for continuous variables and chi-square for dichotomous variables. Cortical thickness analyses were done using generalized linear models, figures 1 and 2 are not cluster corrected to show the full statistical effect, while figure 3 shows the same data with cluster correction and a smaller smoothing kernel of 10 mm FWHM.

3 Results

3.1 Demographics

In total 403 participants from the ADNI data base were used in this analysis. After selecting for AD with AV45 positivity and CDR>0 vs Controls AV45 neg and CDR=0 a total of 300 participants remained. After matching for age and sex 238 participants remained (119 CN ,119AD). After matching AD participants (73.76, SD =8.22) were not significantly older than CN (73.53, SD =6.59), (t=0.2, df=227, p=0.807). The sex distribution between the study groups (53.8% vs 56.6% males, (χ^2=0.07, df=1, p=0.8) was not different. Education level of the CN group was higher (17.2, SD =2.46) compared to the AD group (15.7, SD=2.54) (t=-5, df=235, p<0.001). The percentage of APOE4 carriers was 79.3 % in the AD group and 18.5 %

prevalence of 13.39 for North America (CI up to 17) (Ward et al., 2012) the sample is enriched for homozygous APOE4 in the AD group. The percentage heterozygote APOE4 carriers are in line with reported prevalence for North America. After matching for Age and Sex average and distributions where well matched, while very minor changes in APOE4 distribution were introduced (see table 1). There is no interaction effect of APOE4 by diagnosis on WMSA load (homozygote df=229, p= 0.39, heterozygote df=229, p=0.62). The ADNI population and our sample are predominantly white non-Hispanic (see table 1 for breakdown).

(Table 1 about here)

3.2 Cortical thickness measurement

Figure 1 shows the surface maps of group differences in cortical thickness between the amyloid- CN and amyloid+ AD matched for age and sex. Surface maps of the cortical thickness differences between CN and AD show reduced cortical thickness in AD in several regions including entorhinal cortex, precuneus cortex, superior frontal cortex, pars opercularis, supramarginal gyrus, caudal middle frontal gyrus, lateral occipital cortex (Fig 1. top row) as described in several previous publications (Dickerson et al., 2009; Salat, 2011). When WMSA volume is included in the AD vs CN group differences analysis as a nuisance covariate, differences are greatly reduced to the point where much of the canonical pattern of AD has disappeared with the exception of the parahippocampal, entorhinal region and the cuneus/precuneus (Fig 1. 2nd row).

In a subgroup analysis on AD and CN looking at the effect of WMSA on cortical thickness the pattern is shown in figure 1 (subgroups 3rd row). For CN, WMSA has a significant negative effect on cortical thickness in frontal areas (superior frontal, rostral middle frontal, anterior cingulate, medial and lateral orbitofrontal) as well as showing a relation with WMSA in the temporal pole parts of the superior and middle temporal, supra marginal and inferior parietal regions- several regions overlapping traditional AD regions. For the AD subgroup,

and part of the lingual, notably a positive effect (thickening) on the superior parietal and precuneus was observed- these patterns seem to be complementary to the control patterns in overlap of the full AD effect.

(Figure 1 & 2 about here)

When the CN and AD subgroups are projected back on the group difference map these associations with WSMA have a high overlap with the regions where AD has a lower cortical thickness than CN participants (figure 2). In addition, figure 3 shows the subgroups using a smaller smoothing kernel of 10mm FWHM and cluster correction and placed in the approximate locations that showed consistent regional thinning in AD in multiple samples (Dickerson et al., 2009) coinciding with the temporal pole, entorhinal, fusiform and parahippocampal gyrus.

(Figure 3 about here)

4. Discussion

The current results suggest a reinterpretation of the canonical patterns of cortical thinning in patients with AD that have been described in several prior publications and are typically considered linked to classical AD neuropathology. Controlling group difference for WMSA greatly reduces the effect, showing a widespread effect of vascular pathology in the pattern of AD. Furthermore, subgroup analyses suggest a potential temporal pattern with WMSA contributing to cortical thinning in many typical AD regions in individuals when cognitively intact and amyloid negative, while effect of WMSA on cortical thickness is seen in AD groups in medial temporal and temporal pole areas. Although commonly comorbid, vascular pathology is not a pathology defining feature of AD and is not included in many models of primary AD pathophysiology (in fact, vascular damage can be considered an exclusionary factor for a diagnosis of AD). It may therefore be surprising that there is such a strong link between these measures. Importantly, the controls used in the subgroup analysis were amyloid negative, minimizing the potential for AD pathology to be a substantial contributor to the lesion/thickness associations. Thus, these data provide evidence for a reinterpretation of this assumption of pathologic independence.

Journal Pre-proof

hippocampal volume loss, postmortem tau pathology, as well as worse cognitive performance (Birdsill et al., 2014; Eckerström et al., 2011; McAleese et al., 2015; Rizvi et al., 2018). Other studies have investigated the relation between WMSA and cortical thickness (Jacobs et al., 2014; Seo et al., 2012; Tuladhar et al., 2015) as well as WMSA and Age, but have not previously directly examined the impact of WMSA on AD related thinning and overlap in spatial patterns. The exact role of vascular pathology in AD is currently a topic of debate (Jack et al., 2013; Jagust et al., 2019; Sweeney et al., 2019). The ATN model (Jack et al., 2018) does consider it co-morbidity and independent from AD (but not necessarily from Alzheimer clinical syndrome) but allows for a vascular component to be added. This work expands upon the work of Villeneuve and colleagues that showed similar patterns (but not the parahippocampal region) of cortical thinning in a smaller sample and came to the conclusion that Aβ interacts with vascular risk to enhance cortical thinning in posterior brain regions that are particularly vulnerable to AD (Villeneuve et al., 2014) and Bakkour (Bakkour et al., 2013) comparing a smaller sample of AD with controls. Analyses of the effect of amyloid on cortical thickness showed that the addition of AV45 as a covariate did not appreciably change the presented patterns. We chose not to regress out the effects of age but to match the distributions of equal sized and balanced groups in both age and sex. This ensures that the effect is not driven by group differences in age or sex but does not eliminate the accrual of WMSA over time.

Vascular pathology has long been considered a comorbidity or even fundamental part of AD, and interventions aimed at reducing vascular risk have yielded hope giving results (SPRINT MIND Investigators for the SPRINT Research Group, 2019). Increased WMSA burden has been shown to be associated with typical-AD and Limbic predominant AD-subtypes (Cedres et al., 2020; Ferreira et al., 2018) but less so in minimal atrophy AD suggesting a differential relationship in dementia subtypes. We found a relation of WMSA with CT in frontal regions considered more related to vascular involvement. Importantly we found a significant effect of WMSA in the CN group in many regions typically associated with AD, while in the AD group, the parahippocampal, entorhinal, fusiform and temporal areas are affected by WMSA burden.

Journal Pre-proof

However, we posit, as it is improbable that AD has a protective effect against cortical thickness loss associated with WMSA, it stands to reason that the cortical loss in in a significant part of the canonical pattern of AD has taken place in the time preceding disease onset. Furthermore, it is unlikely that the loss of cortical thickness in the CN group due to WMSA is reversible. We hypothesize that WMSA load associated with cortical thickness in the AD groups is added to the existing damage (and is focused on Alzheimer typical parahippocampal and precuneus regions) and shares variance with AD pathology. The regionally-specific WMSA may be an important pathological component of AD development (Lindemer et al., 2017a). The regions shown in the AD maps are mostly congruent with the non-scaling regions with double blood supply in previous work in our group (Lindemer et al., 2017b) (lateral temporal, lateral orbitofrontal, cuneus, entorhinal and parahippocampal). These regions might be more resistant to WMSA effects and this could explain why they are part of the pattern in the AD group. Together this suggest that accounting for WSMA is important to understand how much of the cortical thickness (and in all probability neural loss) is linked to vascular factors when looking at dementias. While WMSA in different localities might have different underlying pathology, it is possible the co-localization of vascular pathology and AD pathology can interact and amplify via its associated inflammation responses that can have effects beyond the direct vicinity of cerebrovascular damage and negatively affect brain health.

The prevention of damage due to vascular risk factors starting in midlife therefore seems to have merit to retain cortex in the areas at risk in AD.

The use of the large ADNI dataset enabled us to retain adequately sized groups after matching, comparing favorably to previous studies. Careful matching helps in understanding these patterns without controlling for age causing loss of shared variance. Tau pathology is generally linked to cortical thickness(Xia et al., 2017), however the amount of missing data in the CSF p-tau data did not allow for effective matching in this sample.

These results might not generalize to all populations. The ADNI study excludes participants with a Hachinski score of 5 and up, omitting participants with a high likelihood of vascular dementia at baseline. However, counter to what is often stated in literature ADNI does not

the white matter hyperintensity burden in ADNI is lower compared to other cohort studies (Ramirez et al., 2016) , there is sufficient variability in WMSA within the sample.

The ADNI dataset is not a balanced racially diverse sample. Our subset comprises of predominantly (92.86%) white -of which only 5.46% identify as Hispanic-, 0.42 % Native American/Alaskan, 2.94% Asian, 2.52% Black participant which limits. While this does not affect our findings, it does limit the generalizability and hamper our ability to understand the aging and disease processes in more ethnically diverse groups.

Interventions aimed at preventing cortical loss by addressing risk factors for white matter damage in an early could benefit brain health and help preserve cognition in AD and other dementias as well as in aging in general.

5. Conclusions

WSMA are an important factor to consider when investigating patterns of cortical thinning in the context of Alzheimer's disease. A substantial amount of the canonical AD pattern is associated with WMSA load and takes place in both cognitively normal as well as AD participants.

Disclosures

The authors have no relevant conflicts of interests.

Acknowledgments

This work was supported by the National Institutes of Health – NIH (grant number R01NR010827, using resources provided by NIH grants NS042861, NS058793); by the Center for Functional Neuroimaging Technologies (P41RR14075), a P41 Regional Resource supported by the Biomedical Technology Program of the National Center for Research Resources (NCRR), NIH; and by the NCRR Shared Instrumentation Grant Program and/or High-End Instrumentation Grant Program (grant numbers S10RR021110, S10RR023401, S10RR019307, S10RR019254 and S10RR023043). Dr. Mahanand received support from Raman Fellowship awarded by University Grants Commission, Government of India.

Data collection and sharing for this project was funded by the Alzheimer's Disease

DOD ADNI (Department of Defense award number W81XWH-12-2-0012). ADNI is funded by the National Institute on Aging, the National Institute of Biomedical Imaging and Bioengineering, and through generous contributions from the following: AbbVie, Alzheimer's Association; Alzheimer's Drug Discovery Foundation; Araclon Biotech; BioClinica, Inc.; Biogen;Bristol-MyersSquibb Company;CereSpir, Inc.;Cogstate;Eisai Inc.; Elan Pharmaceuticals, Inc.; Eli Lilly and Company; EuroImmun; F. Hoffmann-La Roche Ltd and its affiliated company Genentech, Inc.; Fujirebio; GE Healthcare; IXICO Ltd.; Janssen Alzheimer Immunotherapy Research & Development, LLC.; Johnson & Johnson Pharmaceutical Research & Development LLC.;Lumosity;Lundbeck;Merck & Co., Inc.; Meso Scale Diagnostics, LLC.;NeuroRx Research; Neurotrack Technologies;Novartis Pharmaceuticals Corporation; Pfizer Inc.; Piramal Imaging;Servier; Takeda Pharmaceutical Company; and Transition Therapeutics. The Canadian Institutes of Health Research is providing funds to support ADNI clinical sites in Canada. Private sector contributions are facilitated by the Foundation for the National Institutes of Health (www.fnih.org). The grantee organization is the Northern California Institute for Research and Education, and the study is coordinated by the Alzheimer's Therapeutic Research Institute at the University of Southern California. ADNI data are disseminated by the Laboratory for Neuro Imaging at the University of Southern California.

Journal Pre-proof

CRediT author statement

Joost M. Riphagen: Conceptualization, Writing - Original Draft, Writing - Review & Editing Analyses, Visualization. Mahanand Belathur Suresh: Conceptualization, Analyses, Writing, - Original Draft, Analyses David H. Salat: Conceptualization, Writing - Review & Editing

References

Appelman, A.P.A., Exalto, L.G., van der Graaf, Y., Biessels, G.J., Mali, W.P.T.M., Geerlings, M.I., 2009. White Matter Lesions and Brain Atrophy: More than Shared Risk Factors? A Systematic Review. Cerebrovasc. Dis. 28(3), 227-242.

Bakkour, A., Morris, J.C., Wolk, D.A., Dickerson, B.C., 2013. The effects of aging and Alzheimer's disease on cerebral cortical anatomy: specificity and differential relationships with cognition. Neuroimage 76, 332-344.

Factors influencing accuracy of cortical thickness in the diagnosis of Alzheimer's disease. Hum. Brain Mapp. 39(4), 1500-1515.
Birdsill, A.C., Koscik, R.L., Jonaitis, E.M., Johnson, S.C., Okonkwo, O.C., Hermann, B.P., Larue, A., Sager, M.A., Bendlin, B.B., 2014. Regional white matter hyperintensities: aging, Alzheimer's disease risk, and cognitive function. Neurobiol. Aging 35(4), 769-776.
Brickman, A.M., Guzman, V.A., Gonzalez-Castellon, M., Razlighi, Q., Gu, Y., Narkhede, A., Janicki, S., Ichise, M., Stern, Y., Manly, J.J., Schupf, N., Marshall, R.S., 2015. Cerebral autoregulation, beta amyloid, and white matter hyperintensities are interrelated. Neurosci. Lett. 592, 54-58.
Capizzano, A.A., 2004. White matter hyperintensities are significantly associated with cortical atrophy in Alzheimer's disease. Journal of Neurology, Neurosurgery & Psychiatry 75(6), 822-827.
Cedres, N., Ekman, U., Poulakis, K., Shams, S., Cavallin, L., Muehlboeck, S., Granberg, T., Wahlund, L.O., Ferreira, D., Westman, E., 2020. Brain Atrophy Subtypes and the ATN Classification Scheme in Alzheimer's Disease. Neurodegener. Dis. 20(4), 153-164.
de Leeuw, F.E., de Groot, J.C., Achten, E., Oudkerk, M., Ramos, L.M., Heijboer, R., Hofman, A., Jolles, J., van Gijn, J., Breteler, M.M., 2001. Prevalence of cerebral white matter lesions in elderly people: a population based magnetic resonance imaging study. The Rotterdam Scan Study. J. Neurol. Neurosurg. Psychiatry 70(1), 9-14.
Debette, S., Beiser, A., DeCarli, C., Au, R., Himali, J.J., Kelly-Hayes, M., Romero, J.R., Kase, C.S., Wolf, P.A., Seshadri, S., 2010. Association of MRI markers of vascular brain injury with incident stroke, mild cognitive impairment, dementia, and mortality: the Framingham Offspring Study. Stroke 41(4), 600-606.
Debette, S., Bombois, S., Bruandet, A., Delbeuck, X., Lepoittevin, S., Delmaire, C., Leys, D., Pasquier, F., 2007. Subcortical hyperintensities are associated with cognitive decline in patients with mild cognitive impairment. Stroke 38(11), 2924-2930.
DeCarli., C., Maillard., P., Fletcher., E., 2013. https://adni.bitbucket.io/reference/docs/UCD_ADNI2_WMH/UCD%20ADNI%20II%204%20tissue%20segmentation%20Method.pdf.
Desmarais, P., Gao, A.F., Lanctôt, K., Rogaeva, E., Ramirez, J., Herrmann, N., Stuss, D.T., Black, S.E., Keith, J., Masellis, M., 2021. White matter hyperintensities in autopsy-confirmed frontotemporal lobar degeneration and Alzheimer's disease. Alzheimers Res Ther 13(1), 129.
Dickerson, B.C., Bakkour, A., Salat, D.H., Feczko, E., Pacheco, J., Greve, D.N., Grodstein, F., Wright, C.I., Blacker, D., Rosas, H.D., Sperling, R.A., Atri, A., Growdon, J.H., Hyman, B.T., Morris, J.C., Fischl, B., Buckner, R.L., 2009. The cortical signature of Alzheimer's disease: regionally specific cortical thinning relates to symptom severity in very mild to mild AD dementia and is detectable in asymptomatic amyloid-positive individuals. Cereb. Cortex 19(3), 497-510.
Eckerström, C., Olsson, E., Klasson, N., Bjerke, M., Göthlin, M., Jonsson, M., Rolstad, S., Malmgren, H., Wallin, A., Edman, Å., 2011. High White Matter Lesion Load Is Associated with Hippocampal Atrophy in Mild Cognitive Impairment. Dement. Geriatr. Cogn. Disord. 31(2), 132-138.
Erten-Lyons, D., Woltjer, R., Kaye, J., Mattek, N., Dodge, H.H., Green, S., Tran, H., Howieson, D.B., Wild, K., Silbert, L.C., 2013. Neuropathologic basis of white matter hyperintensity accumulation with advanced age. Neurology 81(11), 977-983.
Ferreira, D., Shams, S., Cavallin, L., Viitanen, M., Martola, J., Granberg, T., Shams, M., Aspelin, P., Kristoffersen-Wiberg, M., Nordberg, A., Wahlund, L.-O., Westman, E., 2018. The contribution of small vessel disease to subtypes of Alzheimer's disease: a study on cerebrospinal fluid and imaging biomarkers. Neurobiol. Aging 70, 18-29.
Journal Pre-proof

2004a. Sequence-independent segmentation of magnetic resonance images. Neuroimage 23 Suppl 1, S69-84.
Fischl, B., van der Kouwe, A., Destrieux, C., Halgren, E., Segonne, F., Salat, D.H., Busa, E., Seidman, L.J., Goldstein, J., Kennedy, D., Caviness, V., Makris, N., Rosen, B., Dale, A.M., 2004b. Automatically parcellating the human cerebral cortex. Cereb. Cortex 14(1), 11-22.
Fletcher, E., Singh, B., Harvey, D., Carmichael, O., DeCarli, C., 2012. Adaptive image segmentation for robust measurement of longitudinal brain tissue change. Conf Proc IEEE Eng Med Biol Soc 2012, 5319-5322.
Garnier-Crussard, A., Bougacha, S., Wirth, M., Dautricourt, S., Sherif, S., Landeau, B., Gonneaud, J., De Flores, R., de la Sayette, V., Vivien, D., Krolak-Salmon, P., Chételat, G., 2021. White matter hyperintensity topography in Alzheimer's disease and links to cognition. Alzheimer's & dementia : the journal of the Alzheimer's Association.
Gattringer, T., Pinter, D., Enzinger, C., Seifert-Held, T., Kneihsl, M., Fandler, S., Pichler, A., Barro, C., Grobke, S., Voortman, M., Pirpamer, L., Hofer, E., Ropele, S., Schmidt, R., Kuhle, J., Fazekas, F., Khalil, M., 2017. Serum neurofilament light is sensitive to active cerebral small vessel disease. Neurology 89(20), 2108-2114.
Godin, O., eacute, lia, Maillard, P., Crivello, F., Alp, eacute, rovitch, A., Mazoyer, B., Tzourio, C., Dufouil, C., 2009. Association of White-Matter Lesions with Brain Atrophy Markers: The Three-City Dijon MRI Study. Cerebrovasc. Dis. 28(2), 177-184.
Hansen, B.B., Klopfer, S.O., 2006. Optimal Full Matching and Related Designs via Network Flows. Journal of Computational and Graphical Statistics 15(3), 609-627.
Ho, D., Imai, K., King, G., Stuart, E.A., 2011. Matchit: Nonparametric Preprocessing for Parametric Causal Inference. 2011 42(8), 28.
Jack, C.R., Jr., Bennett, D.A., Blennow, K., Carrillo, M.C., Dunn, B., Haeberlein, S.B., Holtzman, D.M., Jagust, W., Jessen, F., Karlawish, J., Liu, E., Molinuevo, J.L., Montine, T., Phelps, C., Rankin, K.P., Rowe, C.C., Scheltens, P., Siemers, E., Snyder, H.M., Sperling, R., 2018. NIA-AA Research Framework: Toward a biological definition of Alzheimer's disease. Alzheimer's & dementia : the journal of the Alzheimer's Association 14(4), 535-562.
Jack, C.R., Jr., Knopman, D.S., Jagust, W.J., Petersen, R.C., Weiner, M.W., Aisen, P.S., Shaw, L.M., Vemuri, P., Wiste, H.J., Weigand, S.D., Lesnick, T.G., Pankratz, V.S., Donohue, M.C., Trojanowski, J.Q., 2013. Tracking pathophysiological processes in Alzheimer's disease: an updated hypothetical model of dynamic biomarkers. The Lancet. Neurology 12(2), 207-216.
Jack Jr., C.R., Bernstein, M.A., Fox, N.C., Thompson, P., Alexander, G., Harvey, D., Borowski, B., Britson, P.J., L. Whitwell, J., Ward, C., Dale, A.M., Felmlee, J.P., Gunter, J.L., Hill, D.L.G., Killiany, R., Schuff, N., Fox-Bosetti, S., Lin, C., Studholme, C., DeCarli, C.S., Krueger, G., Ward, H.A., Metzger, G.J., Scott, K.T., Mallozzi, R., Blezek, D., Levy, J., Debbins, J.P., Fleisher, A.S., Albert, M., Green, R., Bartzokis, G., Glover, G., Mugler, J., Weiner, M.W., 2008. The Alzheimer's disease neuroimaging initiative (ADNI): MRI methods. J. Magn. Reson. Imaging 27(4), 685-691.
Jacobs, H.I., Clerx, L., Gronenschild, E.H., Aalten, P., Verhey, F.R., 2014. White matter hyperintensities are positively associated with cortical thickness in Alzheimer's disease. J. Alzheimers Dis. 39(2), 409-422.
Jacobs, H.I., Leritz, E.C., Williams, V.J., Van Boxtel, M.P., van der Elst, W., Jolles, J., Verhey, F.R., McGlinchey, R.E., Milberg, W.P., Salat, D.H., 2013. Association between white matter microstructure, executive functions, and processing speed in older adults: the impact of vascular health. Hum. Brain Mapp. 34(1), 77-95.
Jagust, W., Jack, C.R., Jr., Bennett, D.A., Blennow, K., Haeberlein, S.B., Holtzman, D.M., Jessen, F., Karlawish, J., Liu, E., Molinuevo, J.L., Montine, T., Phelps, C., Rankin, K.P., Rowe,
Journal Pre-proof

"Alzheimer's clinical syndrome" nor "dementia". Alzheimer's & dementia : the journal of the Alzheimer's Association 15(1), 153-157.
Kandel, B.M., Avants, B.B., Gee, J.C., McMillan, C.T., Erus, G., Doshi, J., Davatzikos, C., Wolk, D.A., 2016. White matter hyperintensities are more highly associated with preclinical Alzheimer's disease than imaging and cognitive markers of neurodegeneration. Alzheimers Dement (Amst) 4, 18-27.
Knopman, D.S., Griswold, M.E., Lirette, S.T., Gottesman, R.F., Kantarci, K., Sharrett, A.R., Jack, C.R., Jr., Graff-Radford, J., Schneider, A.L.C., Windham, B.G., Coker, L.H., Albert, M.S., Mosley, T.H., Jr., Investigators, A.N., 2015. Vascular imaging abnormalities and cognition: mediation by cortical volume in nondemented individuals: atherosclerosis risk in communities-neurocognitive study. Stroke 46(2), 433-440.
Landau, S.M., Mintun, M.A., Joshi, A.D., Koeppe, R.A., Petersen, R.C., Aisen, P.S., Weiner, M.W., Jagust, W.J., Alzheimer's Disease Neuroimaging, I., 2012. Amyloid deposition, hypometabolism, and longitudinal cognitive decline. Ann. Neurol. 72(4), 578-586.
Leritz, E.C., Shepel, J., Williams, V.J., Lipsitz, L.A., McGlinchey, R.E., Milberg, W.P., Salat, D.H., 2014. Associations between T1 white matter lesion volume and regional white matter microstructure in aging. Hum. Brain Mapp. 35(3), 1085-1100.
Lindemer, E.R., Greve, D.N., Fischl, B., Augustinack, J.C., Salat, D.H., 2017a. Differential Regional Distribution of Juxtacortical White Matter Signal Abnormalities in Aging and Alzheimer's Disease. Journal of Alzheimer's Disease 57(1), 293-303.
Lindemer, E.R., Greve, D.N., Fischl, B.R., Augustinack, J.C., Salat, D.H., 2017b. Regional staging of white matter signal abnormalities in aging and Alzheimer's disease. NeuroImage: Clinical 14, 156-165.
Lindemer, E.R., Salat, D.H., Smith, E.E., Nguyen, K., Fischl, B., Greve, D.N., 2015. White matter signal abnormality quality differentiates mild cognitive impairment that converts to Alzheimer's disease from nonconverters. Neurobiol. Aging 36(9), 2447-2457.
McAleese, K.E., Firbank, M., Dey, M., Colloby, S.J., Walker, L., Johnson, M., Beverley, J.R., Taylor, J.P., Thomas, A.J., O'Brien, J.T., Attems, J., 2015. Cortical tau load is associated with white matter hyperintensities. Acta neuropathologica communications 3, 60-60.
McAleese, K.E., Miah, M., Graham, S., Hadfield, G.M., Walker, L., Johnson, M., Colloby, S.J., Thomas, A.J., DeCarli, C., Koss, D., Attems, J., 2021. Frontal white matter lesions in Alzheimer's disease are associated with both small vessel disease and AD-associated cortical pathology. Acta Neuropathol.
McAleese, K.E., Walker, L., Graham, S., Moya, E.L.J., Johnson, M., Erskine, D., Colloby, S.J., Dey, M., Martin-Ruiz, C., Taylor, J.P., Thomas, A.J., McKeith, I.G., De Carli, C., Attems, J., 2017. Parietal white matter lesions in Alzheimer's disease are associated with cortical neurodegenerative pathology, but not with small vessel disease. Acta Neuropathol 134(3), 459-473.
McKhann, G.M., Knopman, D.S., Chertkow, H., Hyman, B.T., Jack, C.R., Jr., Kawas, C.H., Klunk, W.E., Koroshetz, W.J., Manly, J.J., Mayeux, R., Mohs, R.C., Morris, J.C., Rossor, M.N., Scheltens, P., Carrillo, M.C., Thies, B., Weintraub, S., Phelps, C.H., 2011. The diagnosis of dementia due to Alzheimer's disease: recommendations from the National Institute on Aging-Alzheimer's Association workgroups on diagnostic guidelines for Alzheimer's disease. Alzheimer's & dementia : the journal of the Alzheimer's Association 7(3), 263-269.
Mortamais, M., Reynes, C., Brickman, A.M., Provenzano, F.A., Muraskin, J., Portet, F., Berr, C., Touchon, J., Bonafe, A., le Bars, E., Maller, J.J., Meslin, C., Sabatier, R., Ritchie, K., Artero, S., 2013. Spatial distribution of cerebral white matter lesions predicts progression to mild cognitive impairment and dementia. PLoS ONE 8(2), e56972.
Journal Pre-proof

Diffusion tensor MRI correlates with executive dysfunction in patients with ischaemic leukoaraiosis. Journal of Neurology, Neurosurgery & Psychiatry 75(3), 441.
O'Sullivan, M., Summers, P.E., Jones, D.K., Jarosz, J.M., Williams, S.C.R., Markus, H.S., 2001. Normal-appearing white matter in ischemic leukoaraiosis: A diffusion tensor MRI study. Neurology 57(12), 2307.
Prins, N.D., Scheltens, P., 2015. White matter hyperintensities, cognitive impairment and dementia: an update. Nature Reviews Neurology 11(3), 157-165.
Provenzano, F.A., Muraskin, J., Tosto, G., Narkhede, A., Wasserman, B.T., Griffith, E.Y., Guzman, V.A., Meier, I.B., Zimmerman, M.E., Brickman, A.M., 2013. White matter hyperintensities and cerebral amyloidosis: necessary and sufficient for clinical expression of Alzheimer disease? JAMA Neurol 70(4), 455-461.
Ramirez, J., McNeely, A.A., Scott, C.J.M., Masellis, M., Black, S.E., 2016. White matter hyperintensity burden in elderly cohort studies: The Sunnybrook Dementia Study, Alzheimer's Disease Neuroimaging Initiative, and Three-City Study. Alzheimer's & Dementia 12(2), 203-210.
Riphagen, J.M., Gronenschild, E., Salat, D.H., Freeze, W.M., Ivanov, D., Clerx, L., Verhey, F.R.J., Aalten, P., Jacobs, H.I.L., 2018. Shades of white: diffusion properties of T1- and FLAIR-defined white matter signal abnormalities differ in stages from cognitively normal to dementia. Neurobiol. Aging 68, 48-58.
Rizvi, B., Lao, P.J., Chesebro, A.G., Dworkin, J.D., Amarante, E., Beato, J.M., Gutierrez, J., Zahodne, L.B., Schupf, N., Manly, J.J., Mayeux, R., Brickman, A.M., 2021. Association of Regional White Matter Hyperintensities With Longitudinal Alzheimer-Like Pattern of Neurodegeneration in Older Adults. JAMA Netw Open 4(10), e2125166.
Rizvi, B., Narkhede, A., Last, B.S., Budge, M., Tosto, G., Manly, J.J., Schupf, N., Mayeux, R., Brickman, A.M., 2018. The effect of white matter hyperintensities on cognition is mediated by cortical atrophy. Neurobiol. Aging 64, 25-32.
Salat, D.H., 2011. The declining infrastructure of the aging brain. Brain Connect 1(4), 279-293.
Seo, S.W., Lee, J.-M., Im, K., Park, J.-S., Kim, S.-H., Kim, S.T., Ahn, H.-J., Chin, J., Cheong, H.-K., Weiner, M.W., Na, D.L., 2012. Cortical thinning related to periventricular and deep white matter hyperintensities. Neurobiol. Aging 33(7), 1156-1167.e1151.
SPRINT MIND Investigators for the SPRINT Research Group, S.-M., 2019. Effect of Intensive vs Standard Blood Pressure Control on Probable Dementia: A Randomized Clinical TrialEffect of Intensive vs Standard Blood Pressure Control on Probable DementiaEffect of Intensive vs Standard Blood Pressure Control on Probable Dementia. JAMA 321(6), 553-561.
Sweeney, M.D., Montagne, A., Sagare, A.P., Nation, D.A., Schneider, L.S., Chui, H.C., Harrington, M.G., Pa, J., Law, M., Wang, D.J.J., Jacobs, R.E., Doubal, F.N., Ramirez, J., Black, S.E., Nedergaard, M., Benveniste, H., Dichgans, M., Iadecola, C., Love, S., Bath, P.M., Markus, H.S., Salman, R.A., Allan, S.M., Quinn, T.J., Kalaria, R.N., Werring, D.J., Carare, R.O., Touyz, R.M., Williams, S.C.R., Moskowitz, M.A., Katusic, Z.S., Lutz, S.E., Lazarov, O., Minshall, R.D., Rehman, J., Davis, T.P., Wellington, C.L., González, H.M., Yuan, C., Lockhart, S.N., Hughes, T.M., Chen, C.L.H., Sachdev, P., O'Brien, J.T., Skoog, I., Pantoni, L., Gustafson, D.R., Biessels, G.J., Wallin, A., Smith, E.E., Mok, V., Wong, A., Passmore, P., Barkof, F., Muller, M., Breteler, M.M.B., Román, G.C., Hamel, E., Seshadri, S., Gottesman, R.F., van Buchem, M.A., Arvanitakis, Z., Schneider, J.A., Drewes, L.R., Hachinski, V., Finch, C.E., Toga, A.W., Wardlaw, J.M., Zlokovic, B.V., 2019. Vascular dysfunction—The disregarded partner of Alzheimer's disease. Alzheimer's & Dementia 15(1), 158-167.
Tuladhar, A.M., Reid, A.T., Shumskaya, E., de Laat, K.F., van Norden, A.G.W., van Dijk, E.J., Norris, D.G., de Leeuw, F.-E., 2015. Relationship Between White Matter Hyperintensities, Cortical Thickness, and Cognition. Stroke 46(2), 425-432.

Alexander, G.E., 2021. Influence of regional white matter hyperintensity volume and apolipoprotein E ε4 status on hippocampal volume in healthy older adults. Hippocampus 31(5), 469-480.
Vernooij, M.W., Ikram, M.A., Vrooman, H.A., Wielopolski, P.A., Krestin, G.P., Hofman, A., Niessen, W.J., Van der Lugt, A., Breteler, M.M., 2009. White matter microstructural integrity and cognitive function in a general elderly population. Arch. Gen. Psychiatry 66(5), 545-553.
Villeneuve, S., Reed, B.R., Madison, C.M., Wirth, M., Marchant, N.L., Kriger, S., Mack, W.J., Sanossian, N., DeCarli, C., Chui, H.C., Weiner, M.W., Jagust, W.J., 2014. Vascular risk and Aβ interact to reduce cortical thickness in AD vulnerable brain regions. Neurology 83(1), 40-47.
Ward, A., Crean, S., Mercaldi, C.J., Collins, J.M., Boyd, D., Cook, M.N., Arrighi, H.M., 2012. Prevalence of apolipoprotein E4 genotype and homozygotes (APOE e4/4) among patients diagnosed with Alzheimer's disease: a systematic review and meta-analysis. Neuroepidemiology 38(1), 1-17.
Wen, W., Sachdev, P.S., Chen, X., Anstey, K., 2006. Gray matter reduction is correlated with white matter hyperintensity volume: a voxel-based morphometric study in a large epidemiological sample. Neuroimage 29(4), 1031-1039.
Xia, C., Makaretz, S.J., Caso, C., McGinnis, S., Gomperts, S.N., Sepulcre, J., Gomez-Isla, T., Hyman, B.T., Schultz, A., Vasdev, N., Johnson, K.A., Dickerson, B.C., 2017. Association of In Vivo [18F]AV-1451 Tau PET Imaging Results With Cortical Atrophy and Symptoms in Typical and Atypical Alzheimer DiseaseAssociation of Cortical Atrophy in AD With [18F]AV-1451 ImagingAssociation of Cortical Atrophy in AD With [18F]AV-1451 Imaging. JAMA Neurology 74(4), 427-436.
Zhao, Y., Gong, C.X., 2015. From chronic cerebral hypoperfusion to Alzheimer-like brain pathology and neurodegeneration. Cell. Mol. Neurobiol. 35(1), 101-110.

Figure 1. Group differences CN-AD and subgroup analyses

Group differences of cognitively normal (CN) and AD participants.
Top row : Threshold at 6 showing areas of cortex thinner in AD compared to CN.
Middle row: Same, but with WMSA load as covariate, Blue is AD thinner than CN red is opposite.
Bottom row : AD and CN Subgroup slope analyses for WMSA load on cortical thickness (threshold all 1.3-2). Blue denotes negative correlation of WSMA load and cortical thickness, red/yellow a positive correlation.

Figure 2. Overlap of WMSA effect on cortical thickness

Overlay of WMSA association with cortical thickness of subgroups projected on the group difference map where the cortex is thinner in AD compared to CN (Yellow). Negative effect of WMSA on cortical thickness in Cyan overlap in Green, Positive in Red, overlap in Orange.

Figure 3. Cortical signature regions and cluster corrected WMSA effect on cortical thickness

Asterisk markers are placed in the approximate locations that showed consistent regional thinning in AD in multiple samples (Dickerson et al., 2009). Correlation between cortical thickness and WSMA load in AD (left) and CN (right) showing significant clusters negatively correlated to WMSA (more WMSA load thinner cortex). The maps have been constructed with a FWHM surface smoothing kernel of 10 mm and cluster corrected for multiple

Journal Pre-proof

p=0.00025(log10(0.00025) =3.61) as teal clusters.

Table 1 demographics

	AD	**CN**	**t- test or χ2**
N	119	119	
Age mean (sd)	73.76 (8.22)	73.53 (6.59)	0.807
Sex males (%)	64 (53.8)	67 (56.6)	0.800
Ethnicity (%)**	113 (95)	112 (94)	0.6
Education (sd)$	15.67 (2.54)	17.15(2.35)	<0.001
MMSE	23.06 (2.11)	29.02 (1.31)	<0.001
CDR=0 (%)	119 (100.0)	0 (0.0)	<0.001
AV45 PET amyloid positive (%)	119 (100.0)	0 (0.0)	<0.001
Mean CSF p-tau (pg/ml)	39.0	19.6	<0.001
Mean WMSA* (cm^3)	7.47	4.08	<0.001
APOE 4 (%)			
Non ε 4 carriers	24 (20.7)	97 (81.5)	<0.001
heterozygous ε 4	64 (55.2)	21 (17.6)	<0.001
homozygous ε 4	28 (24.1)	1 (0.8)	<0.001

Chi Square for dichotomous variables , T-test for continuous variables. (sd)=standard deviation, WMSA* corrected for intracranial volume normalized to average sample ICV, ** White non-Hispanic. MMSE=mini mental state examination, CDR=clinical dementia rating, WMSA=White matter signal abnormalities, APOE=apolipoprotein ε , $ Education in years.

Journal Pre-proof

Verification

The work in this manuscript is not under consideration by another journal, and has not been published previously in whole or substantial part, all authors have contributed significantly to this manuscript, they reviewed the contents of the manuscript being submitted, approve its contents and validate the accuracy of the data. The authors have no relevant conflicts of interest.

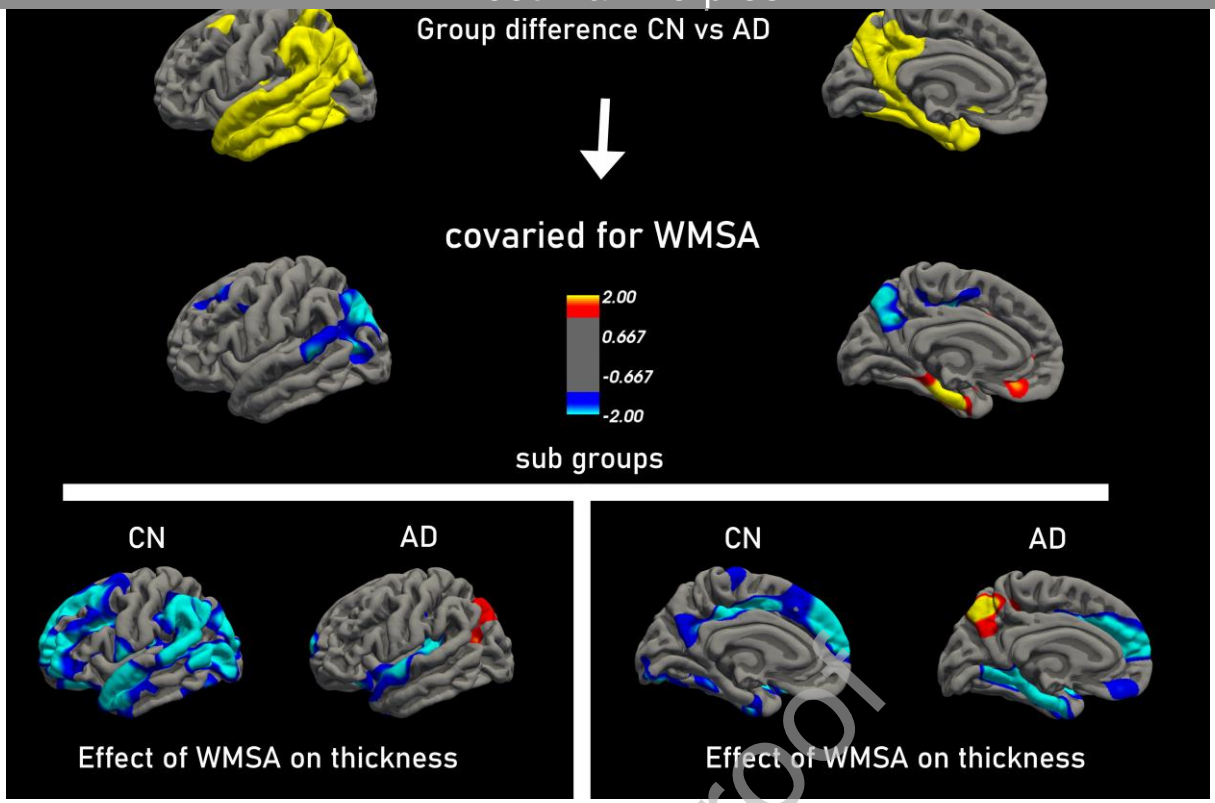

FIG. 1

Journal Pre-proof

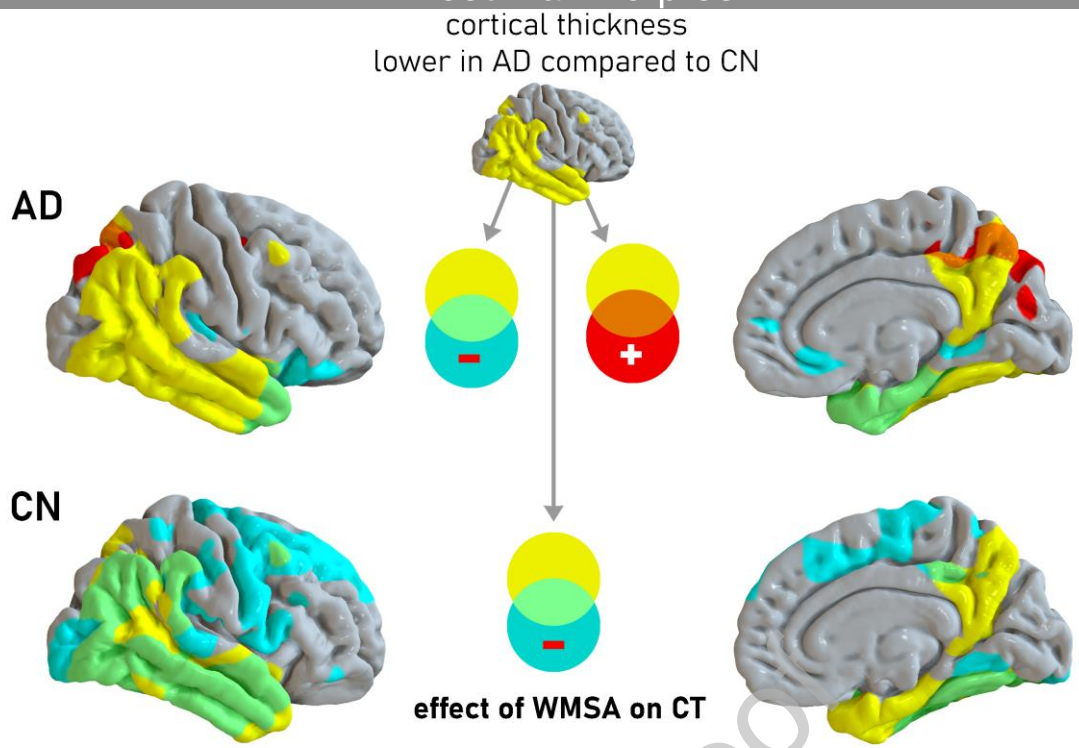

FIG. 2

Journal Pre-proof

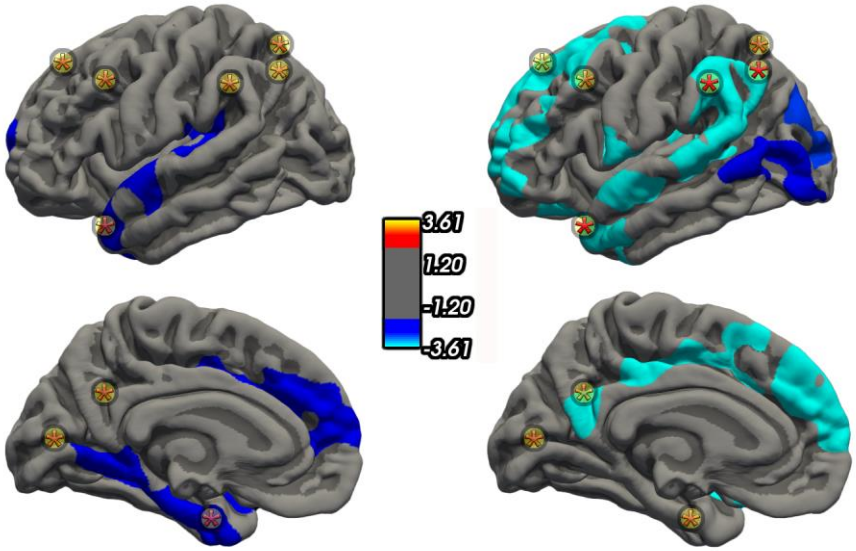

FIG. 3

Journal Pre-proof